

Status of the Experimental Determination of $|V_{ub}|$

Ron Poling

*School of Physics and Astronomy, University of Minnesota,
Minneapolis, MN 55455, USA*

Measurements of the magnitude of the CKM matrix element V_{ub} in inclusive and exclusive semileptonic B -meson decays are reviewed. Theoretical uncertainties in the determination and the prospects for future improvements are discussed.

1 Overview and Motivation

The precise determination of the elements of the Cabibbo-Kobayashi-Maskawa (CKM) matrix^{1,2} is one of the principal goals of the program of testing and refining the Standard Model. In particular, the element V_{ub} , which is directly probed by studies of the charmless semileptonic decay $b \rightarrow ul\nu$, confronts the viability of the Standard Model's description of CP violation. For CP violation in K decays to be accounted for by the phase in the CKM matrix, the magnitudes of all elements must be non zero. In the case of V_{ub} this remained in serious doubt until the first experimental observations of charmless semileptonic decays in mid-1989.

The discovery of $b \rightarrow ul\nu$ was reported almost simultaneously by CLEO³ and ARGUS.⁴ In both cases the evidence came as an excess in inclusive lepton production above the kinematic limit for $b \rightarrow cl\nu$. While these measurements constituted the long-awaited "smoking gun" for non zero V_{ub} , there remained much to be done. Higher-precision confirmation of the inclusive signals was clearly called for. Further theoretical work to reduce the model uncertainty in extracting $|V_{ub}|$ was an even more pressing need. Finally, it was clear that measurement of specific exclusive decay modes for $b \rightarrow ul\nu$ would provide both very compelling confirmation and a complementary avenue of study with different (and conceivably smaller) systematic uncertainties. The past several years have seen significant progress toward achieving these goals.

2 Inclusive Measurement of $b \rightarrow ul\nu$

The measurement of $b \rightarrow ul\nu$ in the inclusive B -meson semileptonic decay momentum spectrum, while conceptually extremely clear-cut, is fraught with serious practical difficulties. The branching fraction for $b \rightarrow ul\nu$ is $\sim 1\%$ of that for $b \rightarrow cl\nu$, and the two spectra overlap over all but the tiny endpoint region above about 2.3 GeV/ c . The B -meson inclusive semileptonic

momentum spectra from CLEO II (shown in Fig. 1 with a fit to the spectator model of Altarelli *et al.*⁵) illustrates the difficulty.

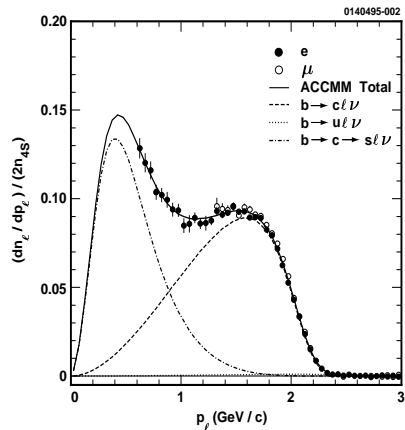


Figure 1: Inclusive B semileptonic momentum spectrum from $2 fb^{-1}$ of CLEO II data. Fit is to the QCD-corrected spectator model of Altarelli *et al.*⁵

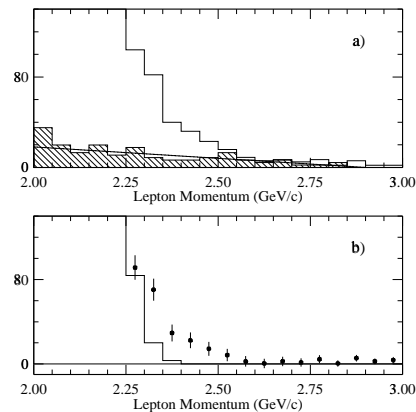


Figure 2: End point of B lepton spectrum from $1 fb^{-1}$ of CLEO II data: a) $\Upsilon(4S)$ (unshaded) and continuum below $B\bar{B}$ threshold (hatched); b) continuum-subtracted spectrum (points) and $b \rightarrow cl\nu$ (histogram).

It is impressive that the data are sufficiently precise that global fits of the spectra to theoretical models of primary and secondary semileptonic decays demand a $b \rightarrow ul\nu$ component (barely visible in Fig. 1). Fitting the overall spectrum is a highly model-dependent procedure, however, and therefore it is preferable to isolate the end-point region and count the yield of leptons in the momentum interval $2.3 - 2.6 GeV/c$. While this range of lepton momenta eliminates most of the $b \rightarrow cl\nu$ contribution, there is a very large continuum background. This must be suppressed with event-shape and other cuts to optimize precision. Model dependence enters in two ways. We are sensitive to the details of the $b \rightarrow ul\nu$ decays in determining the detection efficiency, especially for continuum-suppression procedures which can be strongly q^2 -dependent. Still more serious is the model uncertainty in relating the measured end-point partial branching fraction to the CKM elements.

The best information on inclusive $b \rightarrow ul\nu$ production was presented by CLEO a few years ago, based on the first $1 fb^{-1}$ of CLEO II data.⁶ The excess due to $b \rightarrow ul\nu$ is very clear (Fig. 2), although the signal is somewhat smaller than the discovery measurements had led us to expect. Consideration of several inclusive and exclusive models for $b \rightarrow ul\nu$ leads to $|V_{ub}/V_{cb}| = 0.08 \pm 0.02$,

Table 1: The $|V_{ub}|$ values obtained by normalizing to the B lifetime ($\tau_B = 1.6$ ps). For ARGUS, a partial branching fraction for $b \rightarrow u\ell\nu$ in the momentum range 2.3 – 2.6 GeV/c of $(1.9 \pm 0.4) \times 10^{-4}$ was used. In averaging the squared error was scaled by χ^2/N .

| Model | ARGUS ($\times 10^{-4}$) | CLEO (1990) ($\times 10^{-4}$) | CLEO (1993) ($\times 10^{-4}$) | Average ($\times 10^{-4}$) |
|---------------------|-------------------------------|-------------------------------------|-------------------------------------|---------------------------------|
| KS ¹¹ | 32 ± 3 | 38 ± 6 | 24.9 ± 2.4 | 29 ± 3 |
| WSB ¹² | 43 ± 5 | 48 ± 8 | 34.4 ± 3.3 | 39 ± 4 |
| ACCMM ⁵ | 36 ± 4 | 37 ± 6 | 32.7 ± 3.2 | 34 ± 3 |
| ISGW2 ¹⁰ | 43 ± 5 | 45 ± 8 | 34.3 ± 3.2 | 38 ± 3 |

where model dependence is the primary limitation.

Ritchie Patterson has pointed out it is now possible to extract $|V_{ub}|$ more directly and reliably than by the CLEO and ARGUS ratio procedure.⁷ While determining $|V_{ub}/V_{cb}|$ results in the cancellation of some systematic effects for a single experiment, it introduces unnecessary sensitivity to the model for $b \rightarrow c\ell\nu$. The result has been to exaggerate inconsistencies among the experiments' results for $|V_{ub}|$. Precise measurements of the B -meson lifetime that have been made since the inclusive $b \rightarrow u\ell\nu$ studies now make it preferable to extract $|V_{ub}|^2$ directly through the equation:

$$|V_{ub}|^2 = \frac{\Delta B_u}{\gamma_u f(p) \tau_B}, \quad (1)$$

where ΔB_u is the measured partial branching fraction in the end-point interval, and $f(p)$ and γ_u are model-dependent factors related to the spectral shape (fraction in the specific momentum interval) and overall normalization, respectively. Using $\tau_B = 1.6$ ps as the average B^-/B_d^0 lifetime,⁸ and the published $b \rightarrow u\ell\nu$ results, leads to the values in Table 1. Fig. 3 provides a comparison of the CLEO, ARGUS and CLEO II measurements, both as published and with the τ_B normalization. As expected, the consistency is significantly improved by the revision. The average of the CLEO II results in Table 1 is 0.0032. Both this value and the variations among the different models are consistent with the “standard” value of $|V_{ub}/V_{cb}| = 0.08 \pm 0.02$ with $|V_{cb}| = 0.04$.

3 Exclusive Measurement of $b \rightarrow u\ell\nu$

The measurement of specific charmless final states in semileptonic B decays is the natural next step in the program to refine our knowledge of V_{ub} . Exclusive evidence reinforces our confidence that we understand the source of

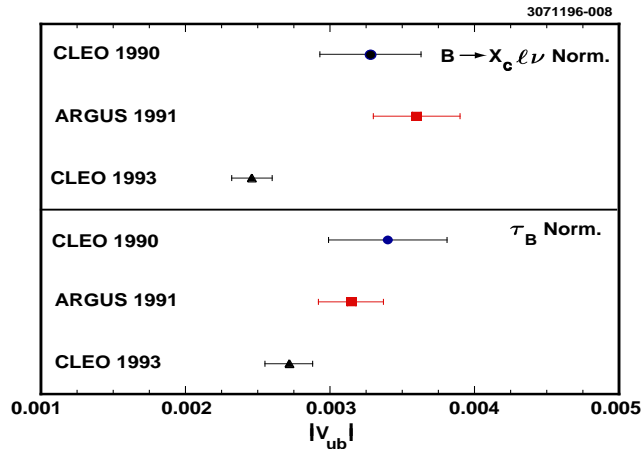


Figure 3: Comparison of CLEO, ARGUS and CLEO II inclusive measurements of $|V_{ub}/V_{cb}| \times 0.04$ and $|V_{ub}|$ as published, and with τ_B normalization as suggested by Patterson.

high-momentum lepton production in B decays. New methods to determine $|V_{ub}|$ bring experimental and theoretical systematic uncertainties that are quite different from the inclusive technique. Furthermore, the detailed information provided by exclusive measurement allows testing and refinement of the theoretical models on which the determination of $|V_{ub}|$ relies.

CLEO presented the first evidence for exclusive charmless semileptonic B decays a few years ago, and has recently published the final version of the analysis.⁹ The technique is full reconstruction of five final states ($B^0 \rightarrow \pi^\mp \ell^\pm \nu$, $B^0 \rightarrow \rho^\mp \ell^\pm \nu$, $B^\pm \rightarrow \pi^0 \ell^\pm \nu$, $B^\pm \rightarrow \rho^0 \ell^\pm \nu$, and $B^\pm \rightarrow \omega \ell^\pm \nu$), where the neutrino is “detected” by careful measurements of missing momentum and energy. The measurement relies on the kinematics of $B\bar{B}$ production at the $\Upsilon(4S)$, with B mesons approximately at rest in the lab and the constraints:

$$\Delta E = E_{ml\nu} - E_{beam} \simeq 0, \text{ and} \quad (2)$$

$$M_{ml\nu} = \sqrt{E_{beam}^2 - |\vec{p}_{ml\nu}|^2} \simeq M_B. \quad (3)$$

The great challenge in this measurement is the reliable determination of the kinematic properties of the neutrino. Key ingredients are CLEO II’s nearly hermetic coverage for both charged tracks (95% of 4π) and photons (98% of 4π), and the development of selection criteria that detect real particles and photons

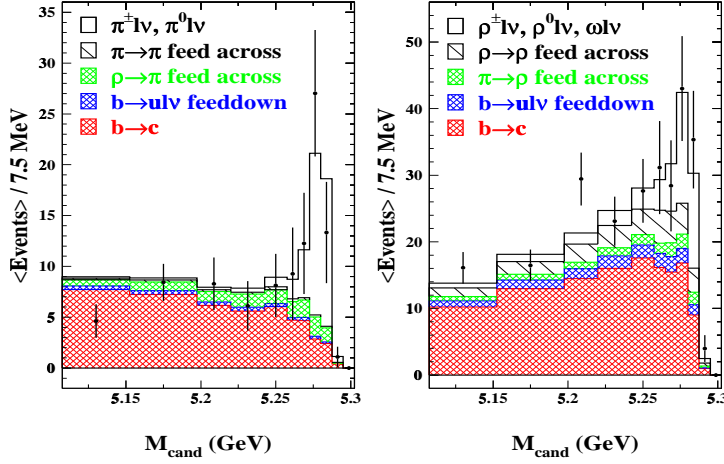


Figure 4: Invariant mass distribution for events in the ΔE signal region for $B \rightarrow \pi\ell\nu$ and $B \rightarrow \rho\ell\nu$. Data points are shown as solid circles and fitted signals are unshaded histograms. Other histograms show background components in fits: $b \rightarrow c\ell\nu$ (large hatch), higher-mass $b \rightarrow u\ell\nu$ (left hatch), $\pi\ell\nu$ feed-across (small hatch), and $\rho\ell\nu$ feed-across (right hatch).

with high efficiency while rejecting spurious ones. To reduce background we reject events in which it can be clearly discerned that some particle or photon was missed: events with more than one lepton detected (and therefore more than one neutrino produced), events with non zero net charge (indicating one or more missed tracks), and events in which the mass of “what’s missing” is not consistent with being a neutrino. The performance of this “neutrino detection” technology is quite good, with a resolution in the neutrino momentum of 110 MeV (about 5%) and in the neutrino direction of 6° . Because the resolution for the neutrino momentum is about 2.5 times better than that for the neutrino energy, we take the neutrino 4-momentum to be $(|\vec{P}_{\text{miss}}|, \vec{P}_{\text{miss}})$.

Even in an exclusive analysis it is necessary to suppress the prodigious $b \rightarrow c\ell\nu$ background by requiring an energetic lepton. The requirements imposed, $p_\ell > 1.5 \text{ GeV}/c$ for $B \rightarrow \pi\ell\nu$ and $p_\ell > 2.0 \text{ GeV}/c$ for $B \rightarrow \rho/\omega\ell\nu$, admit the bulk of the respective spectra, and therefore do not result in as serious model uncertainty as is the case for the end-point measurement. The lower cut value for the $\pi\ell\nu$ decay reflects the softer spectrum for this mode compared to the vector modes.

Distributions of the candidate mass $M_{m\ell\nu}$ are shown in Fig. 4 for combinations which fall in the ΔE signal region, $-0.15 \leq \Delta E < 0.25 \text{ GeV}$. Clear

Table 2: Yields and backgrounds for the five modes, efficiencies found with the ISGW2 model, and fit results. Errors for π^\pm and π^0 , and for ρ^\pm , ρ^0 and ω , are completely correlated.

| Title | π^\pm | π^0 | ρ^\pm | ρ^0 | ω |
|----------------------|----------------|---------------|----------------|----------------|---------------|
| $\Upsilon(4S)$ Yield | 46 | 19 | 47 | 73 | 7 |
| Bkg. | 9.8 ± 2.1 | 1.5 ± 0.5 | 9.5 ± 2.1 | 5.8 ± 1.2 | 0.3 ± 0.8 |
| Efficiency | 0.023 | 0.015 | 0.015 | 0.024 | 0.006 |
| Signal yield | 26.1 ± 6.1 | 8.6 ± 2.0 | 19.5 ± 3.3 | 15.1 ± 2.5 | 3.5 ± 0.6 |
| $b \rightarrow c$ | 7.0 ± 1.2 | 2.9 ± 0.8 | 15.2 ± 1.8 | 21.5 ± 2.2 | 4.6 ± 1.1 |
| $b \rightarrow u$ BG | 0.5 ± 0.1 | 0.2 ± 0.1 | 2.7 ± 0.2 | 2.9 ± 0.2 | 0.5 ± 0.1 |
| crossfeed | 4.1 ± 0.8 | 1.5 ± 0.3 | 4.9 ± 0.9 | 13.4 ± 2.5 | 0.8 ± 0.2 |

signals are apparent above background for both modes. To extract the signals the data are binned coarsely and fitted simultaneously in $M_{m\ell\nu}$, ΔE and (for $\rho/\omega\ell\nu$) in $m_{\pi\pi}$ and $m_{3\pi}$. Isospin and quark-symmetry constraints are assumed ($\Gamma(B^0 \rightarrow \pi^-\ell^+\nu) = 2\Gamma(B^+ \rightarrow \pi^0\ell^+\nu)$, and $\Gamma(B^0 \rightarrow \rho^-\ell^+\nu) = 2\Gamma(B^+ \rightarrow \rho^0\ell^+\nu) = 2\Gamma(B^+ \rightarrow \omega\ell^+\nu)$). From the fit we obtain the yields $N_{\pi\ell\nu}$ and $N_{\rho/\omega\ell\nu}$, and the normalizations for background contributions. The signal shapes are predicted using Monte Carlo simulations for a variety of models, including the updated HQET-consistent quark model of Isgur *et al.* (ISGW2),¹⁰ the relativistic form-factor models of Wirbel, Stech and Bauer (WSB),¹² Körner and Schuler (KS),¹¹ and Melikhov (with five choices of internal parameters),¹³ and a “hybrid” model for which the $\pi\ell\nu$ form factor is taken from Burdman and Kambor¹⁴ and the $\rho\ell\nu$ form factor is from the UKQCD lattice calculation¹⁵ and the form-factor relations of Stech *et al.*¹⁶ Background shapes were obtained by Monte Carlo simulations, and the principal components are $b \rightarrow c\ell\nu$, cross-feed among $b \rightarrow u\ell\nu$ signal modes, and feed-down from higher-mass $b \rightarrow u\ell\nu$ final states as simulated by the ISGW2 model.¹⁰ The data distributions are very well fitted, with a typical value of χ^2 of 145 for 169 d.o.f. The results are summarized in Table 2.

In principle the $B \rightarrow \rho/\omega\ell\nu$ signal could include contributions from non-resonant processes. Examination of the $\pi\pi$ and 3π mass distributions demonstrates that the data are well fitted without nonresonant contributions, which can account for no more than 20% (5%) of the $\rho\ell\nu$ ($\pi\ell\nu$) signal. The yield of $B \rightarrow \omega\ell\nu$ is consistent both with no signal and with a signal of the size expected from the $B \rightarrow \rho\ell\nu$ result.

The opportunity to study details of exclusive charmless semileptonic decays allows significant testing of theoretical models, as well as consistency checks for the interpretation of the signals. The behavior of the $B \rightarrow \pi/\rho/\omega\ell\nu$

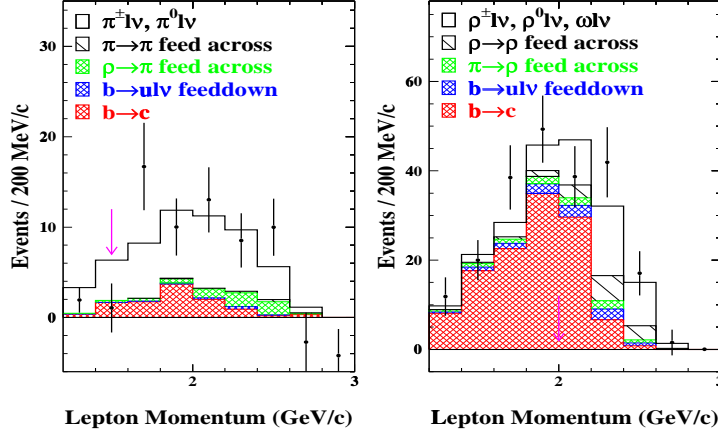


Figure 5: Lepton momentum spectrum for (a) $B \rightarrow \pi l \nu$ and (b) $B \rightarrow \rho l \nu$. Solid circles show data; histograms give backgrounds as identified in caption for Fig. 4.

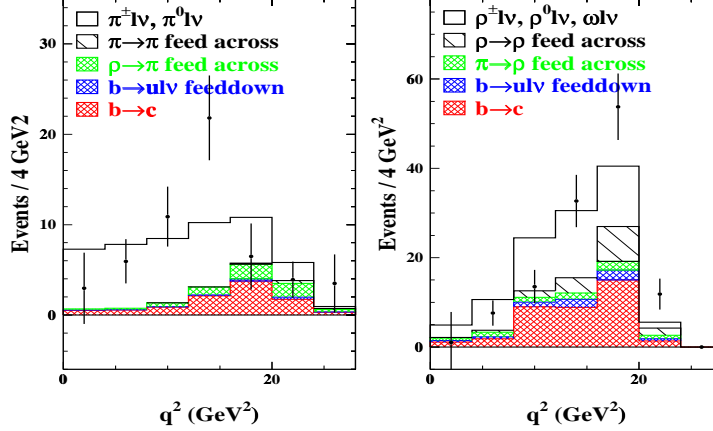


Figure 6: Computed q^2 (mass squared of virtual W) for (a) $B \rightarrow \pi l \nu$ and (b) $B \rightarrow \rho l \nu$. Solid circles show data; histograms give backgrounds as identified in caption for Fig. 4.

signal is consistent with theoretical expectations, as simulated with the CLEO II Monte Carlo. This is demonstrated by data/Monte Carlo comparisons for several distributions, including lepton momentum (Fig. 5) and q^2 (Fig. 6).

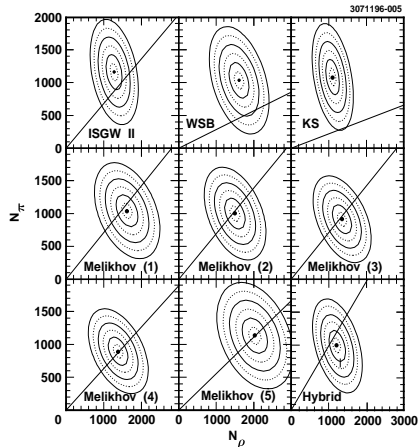


Figure 7: Contours of number of $\pi\ell\nu$ decays versus number of $\rho\ell\nu$ decays with predictions (diagonal lines) for several models.

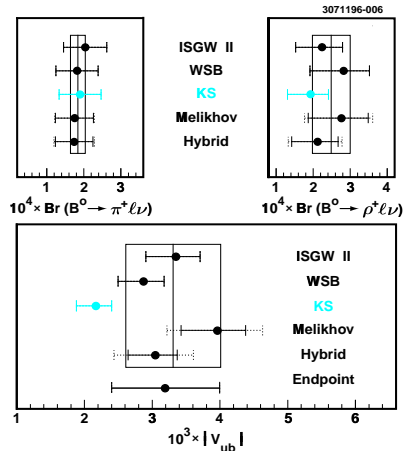


Figure 8: Results of CLEO's measurements of branching fractions for exclusive charmless semileptonic B decays and $|V_{ub}|$.

Fig. 7 gives a concrete example of how the exclusive measurements can be used to exclude particular theoretical models. For each model there is a prediction of the pseudoscalar/vector ratio that can be confronted with the observed proportions of $B \rightarrow \pi\ell\nu$ and $B \rightarrow \rho\ell\nu$. All models considered are found to be consistent with the data, except for KS, which is ruled out with 99.5% confidence and is therefore excluded from further consideration.

CLEO results for the branching fractions for exclusive charmless semileptonic decays and for measurements of $|V_{ub}|$ from both inclusive and exclusive studies are summarized in Fig. 8. There is excellent agreement among the models that are consistent with the observed pseudoscalar/vector ratio. Averaging over these models, we find the following:

$$\mathcal{B}(B^0 \rightarrow \pi^- \ell^+ \nu) = (1.8 \pm 0.4 \pm 0.3 \pm 0.2) \times 10^{-4} \quad (4)$$

$$\mathcal{B}(B^0 \rightarrow \rho^- \ell^+ \nu) = (2.5 \pm 0.4^{+0.5}_{-0.7} \pm 0.5) \times 10^{-4} \quad (5)$$

$$|V_{ub}| = (0.0033 \pm 0.0002^{+0.0003}_{-0.0004} \pm 0.0007) \quad (6)$$

where the errors are statistical, experimental systematic, and model-dependent systematic, respectively. For the value of $|V_{ub}|$ there is strikingly good agreement with the inclusive result.

4 Conclusions and Prospects for Future Improvements

Our knowledge of $|V_{ub}|$ has improved significantly in the past several years, with inclusive and exclusive measurements both giving the result $|V_{ub}| \sim 3 \times 10^{-3}$, with overall uncertainties of about 25%. The need and potential for continuing progress is great. New or updated CLEO inclusive and exclusive studies are under way, with much more data and improved analysis procedures. While the impressive agreement between inclusive and exclusive determinations of $|V_{ub}|$ reinforces our confidence that we are on the right track, it is clear that redoubled efforts to reduce theoretical uncertainties are required. Some approaches to this are purely theoretical, while others involve better use of data to constrain, exclude, or otherwise guide improvements in the models. More data and better detectors, especially as we embark on the era of the three B factories, will be the key.

An example of a more ambitious analysis that seeks inoculation against at least some model uncertainty was presented by ALEPH at the 1996 ICHEP in Warsaw.¹⁷ To distinguish $b \rightarrow u\ell\nu$ from $b \rightarrow c\ell\nu$ over the full momentum range, ALEPH uses sophisticated neural-net procedures that exploit the advantages of vertex tagging with boosted B 's at the Z^0 . While the technique appears promising, and initial results are consistent with measurements at the $\Upsilon(4S)$, it is clear that systematic uncertainties (especially in the modeling of the $b \rightarrow c\ell\nu$ background) are severe. It is to be hoped that these uncertainties can be mastered, so that higher energy measurements can add significantly to our knowledge of $|V_{ub}|$.

Overall, while we can be impressed with the progress so far, we can rest assured that the appetite for improved precision in $|V_{ub}|$ will remain strong for the foreseeable future.

Acknowledgments

I would like to thank the organizers for the opportunity to participate in a most enjoyable and informative conference. The CLEO research described here has been made possible by the outstanding efforts of the CESR accelerator staff, and continuing support from the U.S. Department of Energy and the National Science Foundation.

References

1. N. Cabibbo, *Phys. Rev. Lett.* **10**, 531 (1963).
2. M. Kobayashi and T. Maskawa, *Prog. Theor. Phys.* **49**, 652 (1973).

3. R. Fulton *et al.* (CLEO collaboration), *Phys. Rev. Lett.* **64**, 16 (1990).
4. H. Albrecht *et al.* (ARGUS collaboration), *Phys. Lett.B* **234**, 409 (1990);
H. Albrecht *et al.* (ARGUS collaboration), *Phys. Lett.B* **255**, 297 (1991).
5. G. Altarelli *et al.*, *Nucl. Phys. B* **208**, 365 (1982).
6. J. Bartelt *et al.* (CLEO collaboration), *Phys. Rev. Lett.* **71**, 4111 (1993).
7. J.R. Patterson in *Proceedings of the 28th International Conference on High-Energy Physics*, Warsaw, Poland, Z. Ajduk and A.K. Wroblewski, eds., World Scientific (1997).
8. Thomas R. Junk, these proceedings.
9. J.P. Alexander *et al.* (CLEO Collaboration), *Phys. Rev. Lett.* **77**, 5000 (1996).
10. N. Isgur and D. Scora, *Phys. Rev. D* **52**, 2783 (1995).
11. J. Körner and G. Schuler, *Z. Phys. C* **38**, 511 (1988).
12. M. Wirbel, B. Stech and M. Bauer, *Z. Phys. C* **29**, 637 (1985).
13. D. Melikhov, *Phys. Rev. D* **53**, 2160 (1996).
14. G. Burdman and J. Kambor, *PRD* **55**, 2817 (1997).
15. J.M. Flynn *et al.*, *Nucl. Phys. B* **461**, 327 (1996); J.M. Flynn *et al.*, *Nucl. Phys. B* **476**, 313 (1996).
16. B. Stech *et al.*, *Phys. Lett.B* **354**, 447 (1995).
17. ALEPH collaboration, contributed paper PA05-59 to the 28th International Conference on High-Energy Physics, Warsaw, Poland, July 1996.